Flavour Changing Neutral Current decays at LHCb

Carla Marin carla.marin@cern.ch
on behalf of the LHCb collaboration

Moriond EW 2025

UNIVERSITAT DE BARCELONA

European Research Council
Established by the European Commission

Content

- Introduction
- Angular analyses:
  - Analysis of $\Lambda_b \to pK\mu^+\mu^-$ decays
  - Comprehensive analysis of local and nonlocal amplitudes in the $B^0 \to K^*\mu^+\mu^-$ decay
  - Angular analyses with electrons
- Lepton Flavour Universality (LFU) tests:
  - Test of Lepton Flavour Universality with $B_s \to \Phi l^+l^-$ decays
  - Test of Lepton Flavour Universality with $B^+ \to K^+\pi^+\pi^-l^+l^-$
  - Measurement of the branching fraction ratio R_K at large dilepton invariant mass

See also A. Scarabotto's talk on lepton flavour violation, rare charm & strange decays

Flavour Changing Neutral Currents (FCNC)

- Only at loop level in SM → sensitive to effects of New Physics (NP) in the loops and access to larger scales than direct searches
- LHCb: tests of couplings to 3rd generation b-quarks in b → sll decays
- b → sll decays suppressed by smallness of $V_{tb}V_{ts}$

$$V_{\mathrm{CKM}} = \begin{pmatrix} V_{ud} & V_{us} & V_{ub} \\ V_{cd} & V_{cs} & V_{cb} \\ V_{td} & V_{ts} & V_{tb} \end{pmatrix}$$

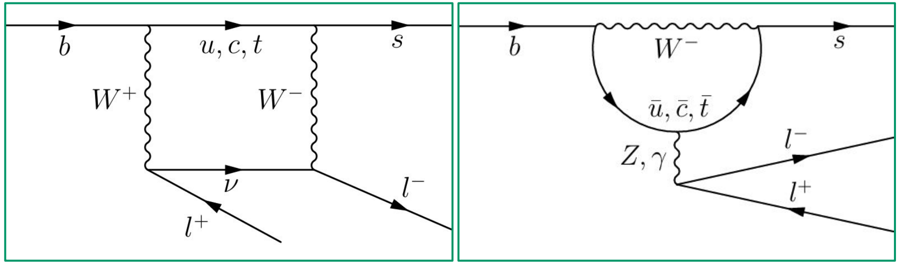

SM

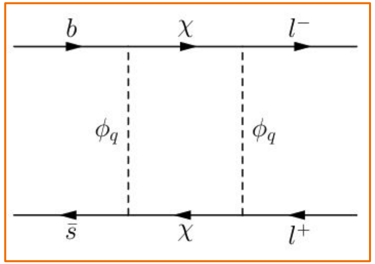

NP

FCNC observables

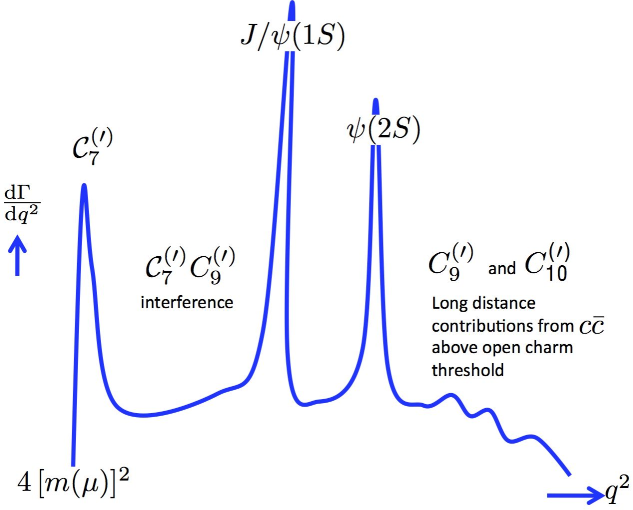

Complementary sensitivity to NP in:

- Leptonic, semileptonic and radiative decays
  - semileptonic: different $q^2 = (m_{ll})^2$ regions
- different observables:
  - Branching fractions (BF): predictions affected by hadronic uncertainties
  - Angular observables: first-order uncertainty cancellations
  - Ratios of BF: large uncertainty cancellation

$$H_{eff} \propto V_{tb} V_{ts}^* \sum_i \left(C_i \mathcal{O}_i + C_i' \mathcal{O}_i' \right)$$

C_i = Wilson coefficients

$$O_7^{(\prime)} \propto (\bar{s}\sigma_{\mu\nu} P_{R(L)} b) F^{\mu\nu}$$
$$O_9^{(\prime)} \propto (\bar{s}\gamma_\mu P_{L(R)} b)(\bar{l}\gamma_\mu l)$$
$$O_{10}^{(\prime)} \propto (\bar{s}\gamma_\mu P_{L(R)} b)(\bar{l}\gamma_\mu\gamma_5 l)$$
$$O_S^{(\prime)} \propto (\bar{s} P_{L(R)} b)(\bar{l}\, l)$$
$$O_P^{(\prime)} \propto (\bar{s} P_{L(R)} b)(\bar{l}\gamma_5 l)$$

LHCb: Large Hadron Collider Beauty experiment

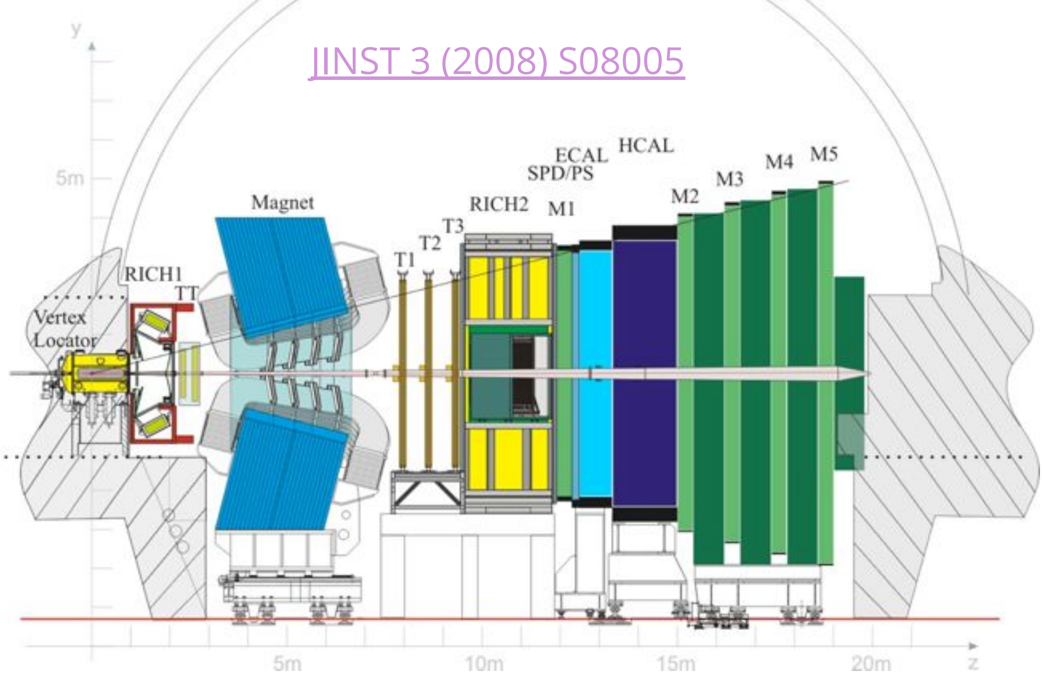

JINST 3 (2008) S08005

- Run 1 (2010-2012) ~ 3 fb^{-1}
- Run 2 (2015-2018) ~ 6 fb^{-1}

$\Delta p/p$ = 0.5 - 1.0%
ΔIP = (15 +29/p_T[GeV]) μm

$\Delta E/E_{ECAL}$ = 1% + 10% / √(E[GeV])

Electron ID ~90%
for ~5% e→h mis-id probability

Kaon ID ~ 95%
for ~ 5% π→K mis-id probability

Muon ID ~ 97%
for 1-3% π→μ mis-id probability

Int.J.Mod.Phys.A30,1530022(2015)

b → sll anomalies

Hints for deviations wrt SM in b → s$\mu^+\mu^-$ BR and angular observables.
A lot of interest due to coherence and combined significance.

$B^0 \to Kl^+l^-$

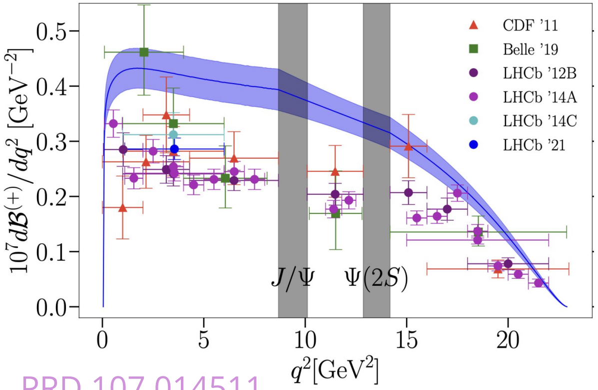

PRD.107.014511

$B_s^0 \to \varphi\mu^+\mu^-$

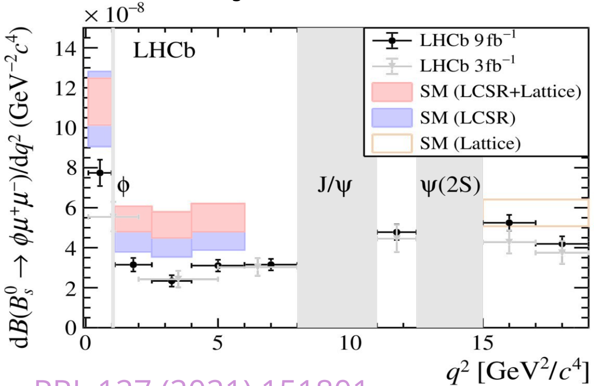

PRL 127 (2021) 151801

$B^0 \to K^*\mu^+\mu^-$

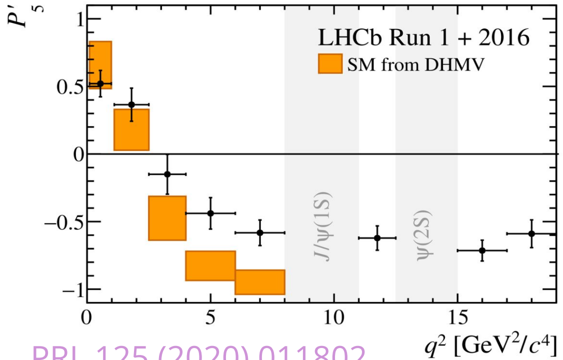

PRL 125 (2020) 011802
Also CMS, Atlas, Belle

Open question: NP (in C_9/C_{10}) or non-local SM hadronic effects, eg charm-loop?

Analysis of $\Lambda_b \to pK\mu^+\mu^-$ decays

JHEP 12 (2024) 147

JHEP 12 (2024) 147

Strategy

Measurement of $\Lambda_b \to pK\mu^+\mu^-$ BF and angular coefficients in q^2 and m(pK) bins

- q^2: 0.10 - 17.5 GeV^2, excluding Φ and ψ(2S); J/ψ as control
- m(pK): 1.4359 - 5.41 GeV, including many $\Lambda \to pK$ resonances with different J^P

5-dimensional decay rate:

$$\frac{d^5\Gamma}{d\mathbf{\Phi}} = \frac{3}{8\pi}\sum_{i=1}^{46} K_i(q^2, m_{pK}^2) f_i(\mathbf{\Omega})$$

$\Phi = (q^2, m_{pK}, \cos\theta_\mu, \cos\theta_p, \phi)$

- treat Λ_b as unpolarised and include $J_\Lambda \leq 5/2 \Rightarrow$ 46 angular terms
- differential BF wrt J/ψ mode
- K_i angular coefficients from moments of angular distribution:

$$\overline{K}_i = \frac{1}{N}\sum_{\text{event } n} w(\mathbf{\Phi}_n) f_i(\mathbf{\Omega}_n)$$

ω: detector efficiency & background subtraction

JHEP 12 (2024) 147

$\Lambda_b \to pK\mu^+\mu^-$ results

Overall compatible with SM. Better understanding of hadronic system needed for detailed interpretation.

Differential BF in (q^2, m_{pK}) bins

- limited by BF($\Lambda_b \to pK\,J/\psi$) knowledge
- first m_{pK} bin compatible with $\Lambda_b \to \Lambda(1520)\,\mu^+\mu^-$
- q^2 shape not compatible with SM quark-model
- m_{pK} shape similar to $\Lambda_b \to pK\,J/\psi$ and $\Lambda_b \to pK\gamma$, consistent with available phase-space

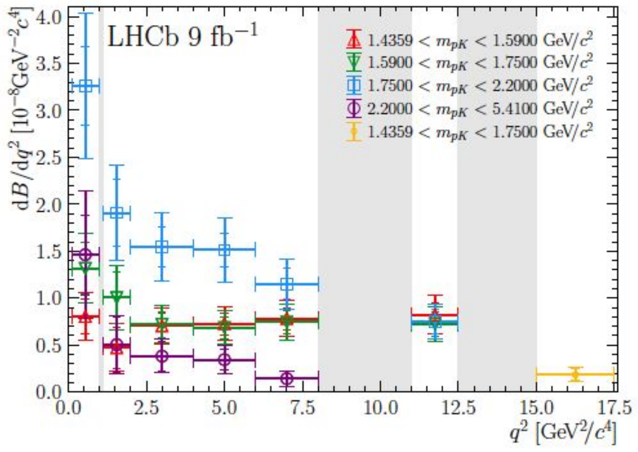

JHEP 12 (2024) 147

$\Lambda_b \rightarrow pK\mu^+\mu^-$ results

Overall compatible with SM. Better understanding of hadronic system needed for detailed interpretation.

Differential BF in (q^2, m_{pK}) bins

- limited by BF($\Lambda_b \rightarrow pK\, J/\psi$) knowledge
- first m_{pK} bin compatible with $\Lambda_b \rightarrow \Lambda(1520)\, \mu^+\mu^-$
- q^2 shape not compatible with SM quark-model
- m_{pK} shape similar to $\Lambda_b \rightarrow pK\, J/\psi$ and $\Lambda_b \rightarrow pK\gamma$, consistent with available phase-space

Complete set of angular observables:

- A^{μ}_{FB}: sign-change low and high q^2 → vector and axial-vector interference
- large A^{p}_{FB} → interference Λ states
- tabulated values in q^2 and m_{pK} provided

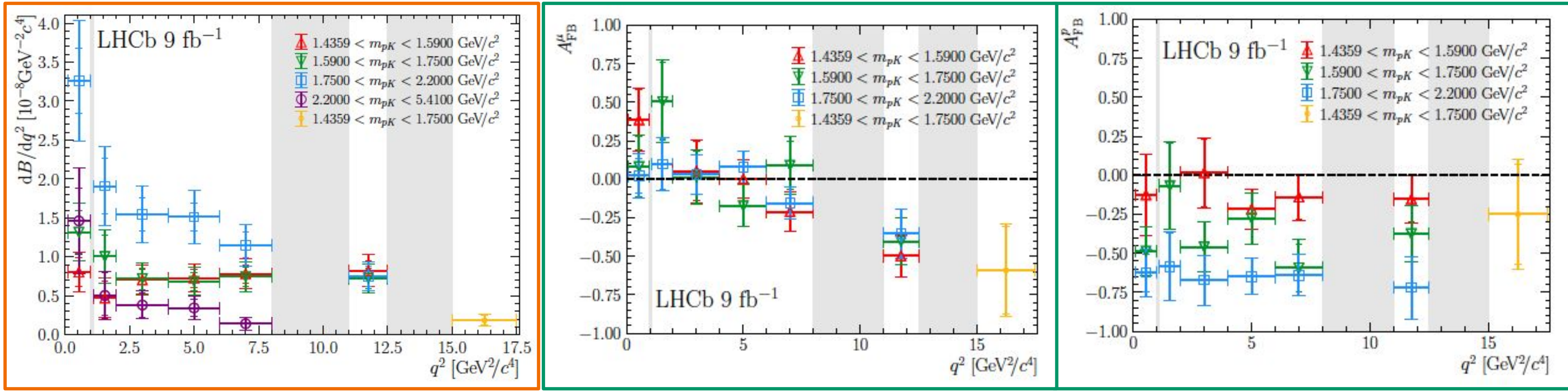

Comprehensive analysis of local and nonlocal amplitudes in the $B^0 \to K^*\mu^+\mu^-$ decay

JHEP 09 (2024) 026

JHEP 09 (2024) 026

New approach to $B^0 \longrightarrow K^*\mu^+\mu^-$ angular analysis

Previously: exclude J/ψ and ψ(2S); effect on rare mode from theory estimates

Here: fit full q^2 and measure local and nonlocal amplitudes from data

- acceptance & resolution from MC
- background fraction from mass fit

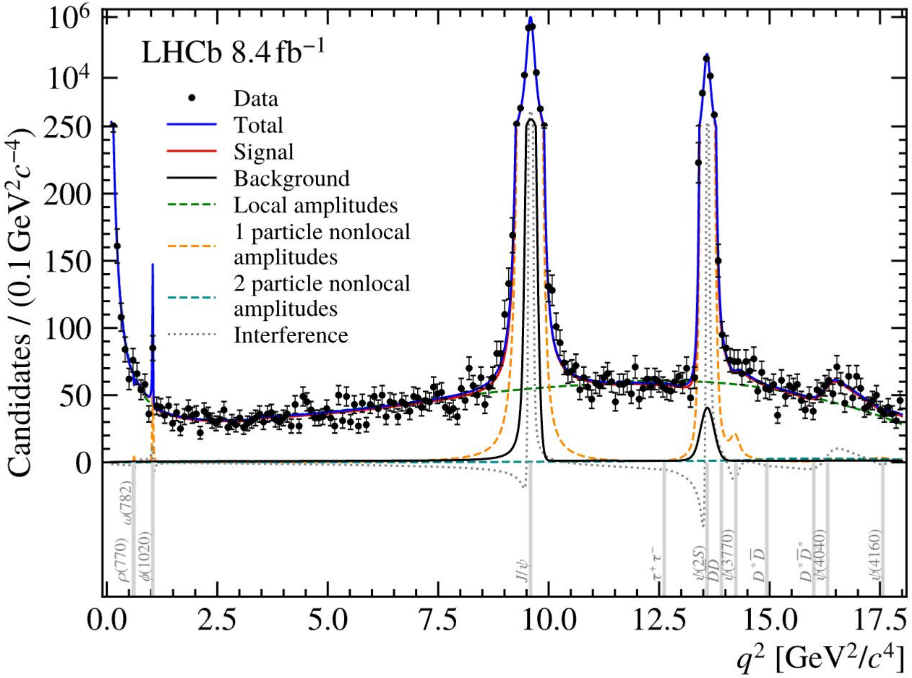

Extraction of local and nonlocal amplitudes

Fit 4-dimensional decay rate, with 796 < m(Kπ) < 996 MeV:

$$\frac{d^4 \overset{(-)}{\Gamma}(B^0 \to K^+\pi^-\mu^+\mu^-)}{dq^2\, d\vec{\Omega}} = \frac{9}{32\pi} \sum_i \overset{(-)}{J}_i(q^2) f_i(\cos\theta_\ell, \cos\theta_K, \phi) G_i$$

- $f_i(\Omega)$: spherical harmonic angular coefficients
- G_i: line-shape of Kπ system (including P- and S-wave)
- $J_i(q^2)$: functions of C_i and local hadronic form-factors
- nonlocal effects absorbed as shift to C_9: $\mathcal{C}_9^{(\mathrm{eff}),\lambda} = \mathcal{C}_9 + Y_{q\bar{q},\lambda}(q^2)$
  - one-particle $\{\rho(770), \omega(782), \phi(1020), J/\psi, \psi(2S), \psi(3770), \psi(4040), \psi(4160)\}$
  - two-particle $\{D\overline{D}, D^*\overline{D}, D^*\overline{D}^*\}$

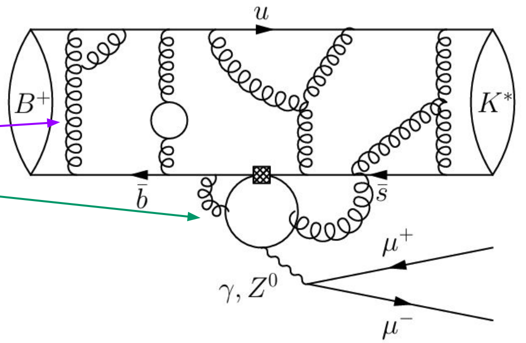

JHEP 09 (2024) 026

$B^0 \to K^* \mu^+ \mu^-$ results

- Measure contribution one- and two-particle nonlocal amplitudes across q^2
- Measurement of $C^{(\prime)}_9$ and $C^{(\prime)}_{10}$ Wilson coefficients: still 2.1σ deviation wrt SM in C_9
- Postfit local form factors compatible with priors, but results sensitive to priors → improved calculations needed
- First measurement of $C_{9\tau}$ from $b \to s\tau^+\tau^-$, $\tau^+\tau^- \to \gamma^* \to \mu^+\mu^-$: $|C_{9\tau}| < 500$ at 90% CL

Wilson Coefficient results	
$\mathcal{C}_9$	$3.56 \pm 0.28 \pm 0.18$
$\mathcal{C}_{10}$	$-4.02 \pm 0.18 \pm 0.16$
$\mathcal{C}_9'$	$0.28 \pm 0.41 \pm 0.12$
$\mathcal{C}_{10}'$	$-0.09 \pm 0.21 \pm 0.06$
$\mathcal{C}_{9\tau}$	$(-1.0 \pm 2.6 \pm 1.0) \times 10^2$

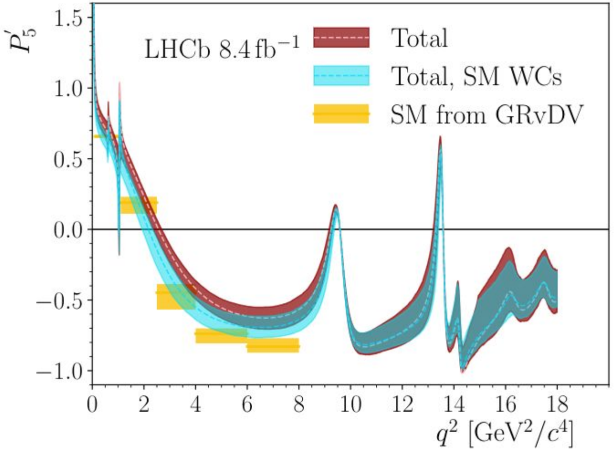

Angular analyses with electrons

Allow Lepton Universality tests in angular coefficients and give access to very low q^2 testing C_7

See M. Hartman and L. Paolucci YSF talks this afternoon for recent results on $B^0 \to K^{*}e^{+}e^{-}$ and $B_s \to \Phi e^{+}e^{-}$

JHEP 03 (2025) 047
arXiv:2502.10291
LHCb-PAPER-2025-006 in preparation

Lepton Flavour Universality tests

Leptons of different species couple identically to electroweak bosons in SM
Accidental symmetry → not necessarily realised in BSM scenarios

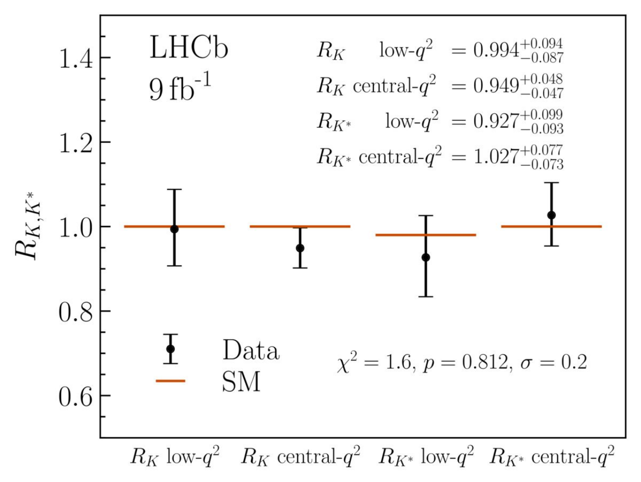

PRD 108 (2023) 032002

Lepton Flavour Universality (LFU) tests

Measure ratio of same b → sll process with muons and electrons in final state:
Hadronic uncertainties cancel in ratio → very clean theory prediction

$$R_H \equiv \frac{\int \frac{d\Gamma(B \to H\mu^+\mu^-)}{dq^2} dq^2}{\int \frac{d\Gamma(B \to He^+e^-)}{dq^2} dq^2}$$

Experimentally:

$$R_H \propto \underbrace{\frac{N(B \to H\mu^+\mu^-)}{N(B \to He^+e^-)}}_{\text{events}} \times \underbrace{\frac{\epsilon(B \to He^+e^-)}{\epsilon(B \to H\mu^+\mu^-)}}_{\text{efficiency}}$$

events: count in experiment

efficiency: from simulation and calibration samples

Challenges:

- e and μ behave very differently
- hard to estimate efficiencies
  ⇒ double-ratio wrt B → H J/ψ control modes

arXiv:2410.13748

LFU with $B_s \rightarrow \phi l^+ l^-$ decays

First LFU test in B_s system:

- same strategy as previous LFU tests
- low background thanks to narrow Φ state → include high q^2 for first time at LHCb
    - more challenging bkgs at high q^2 → dedicated BDT and fit model

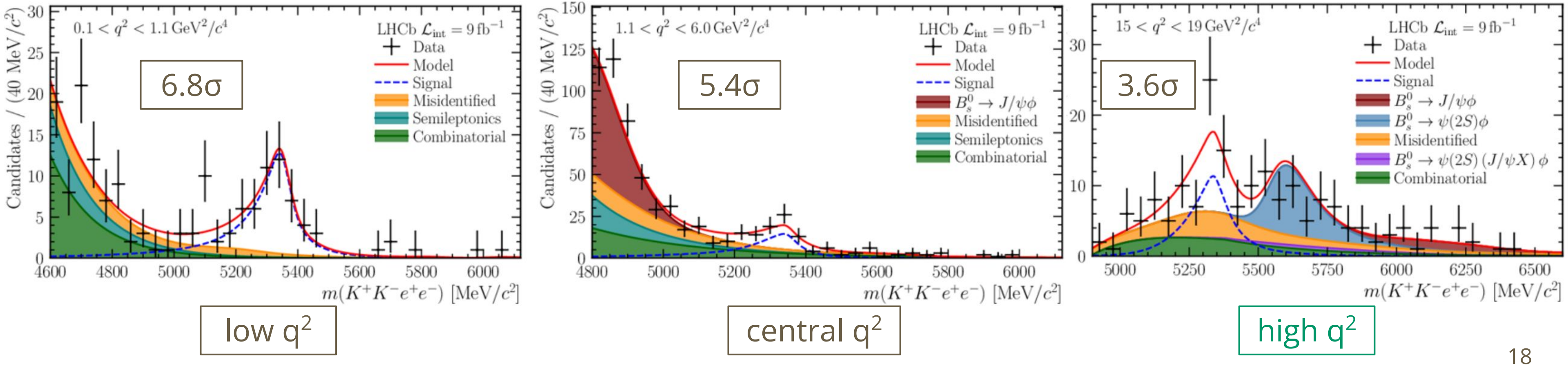

arXiv:2410.13748

LFU with $B_s \longrightarrow \varphi l^+ l^-$ decays

Results:

- first observation of $B_s \to \varphi\, e^+e^-$ at low and central q^2 and measurement of BF
- LFU results compatible with previous measurements and SM
  - most precise measurement at high q^2

q^2 [GeV$^2/c^4$]	R_ϕ^{-1}	$\mathrm{d}\mathcal{B}(B_s^0 \to \phi e^+e^-)/\mathrm{d}q^2$ [10^{-7} GeV$^{-2}c^4$]
$0.1 < q^2 < 1.1$	$1.57^{+0.28}_{-0.25} \pm 0.05$	$1.38\ ^{+0.25}_{-0.22} \pm 0.04 \pm 0.19 \pm 0.06$
$1.1 < q^2 < 6.0$	$0.91^{+0.20}_{-0.19} \pm 0.05$	$0.26 \pm 0.06 \pm 0.01 \pm 0.01 \pm 0.01$
$15.0 < q^2 < 19.0$	$0.85^{+0.24}_{-0.23} \pm 0.10$	$0.39 \pm 0.11 \pm 0.04 \pm 0.02 \pm 0.02$

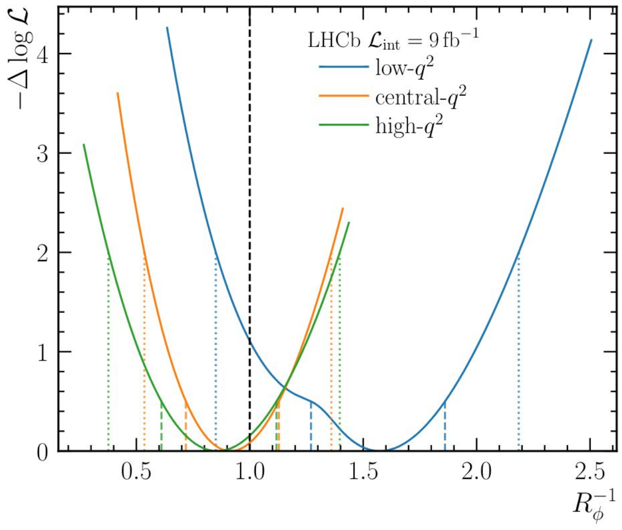

Statistically dominated
BF systematics: internal, $dB(B_s\to\Phi\mu^+\mu^-)/B(B_s\to\Phi J/\psi)$, $B(B_s\to\Phi J/\psi)$

arXiv:2412.11645

LFU with $B^+ \to K^+\pi^+\pi^- l^+ l^-$ decays

First LFU test in this decay, following strategy of previous measurements

- inclusive measurement in $1.1 < m(K\pi\pi) < 2.4$ GeV and $1.1 < q^2 < 7$ GeV^2
- first observation of $B^+ \to K\pi\pi e^+ e^-$, exceeding 10σ significance
- LFU results compatible with SM

$$R^{-1}_{K\pi\pi} = 1.31^{+0.18}_{-0.17}\,(\text{stat})\,^{+0.12}_{-0.09}\,(\text{syst})$$

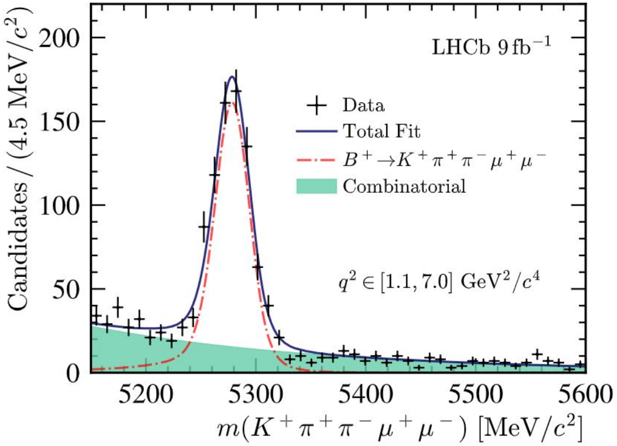

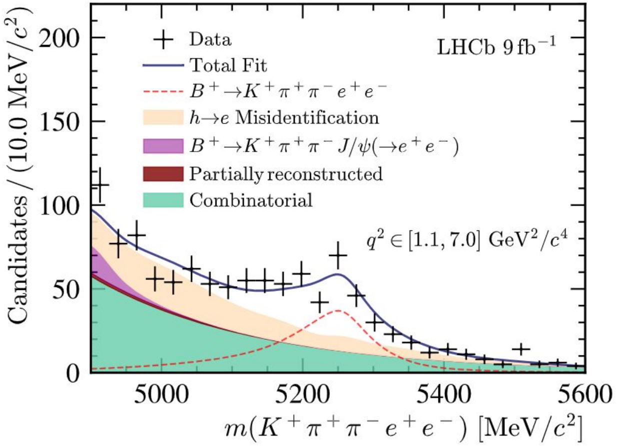

R_K at large dilepton invariant mass

R_K measurement at $q^2 > 14.3$ GeV^2

- optimised selection and background studies for this q^2 region
- most precise LFU measurement above ψ (2S) region
- Results compatible with SM

$$R_K(q^2 > 14.3\ \mathrm{GeV}^2/c^4) = 1.08^{+0.11}_{-0.09}{}^{+0.04}_{-0.04}$$ Preliminary

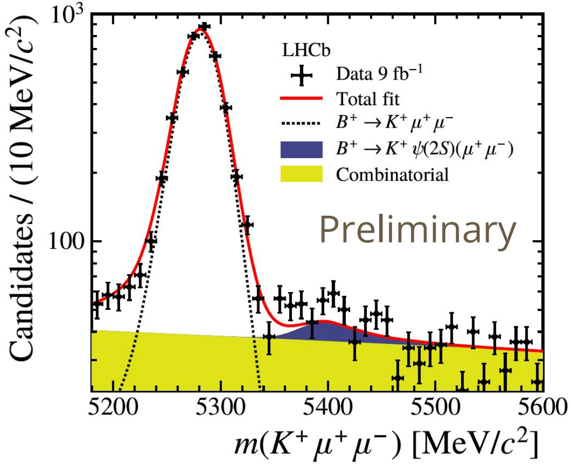

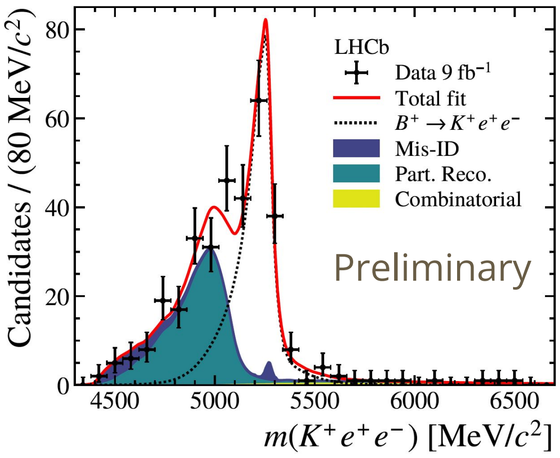

Outlook

LHCb completing FCNC results with full Run 2 dataset, still statistically limited

Major upgrade for Run 3: >8 fb^{-1} in 2024 with improved trigger efficiency. Expect even more in 2025 and aim to reach 300 fb^{-1} in Run 5 with Upgrade 2.

Precision of $b \to sll$ decays will be hugely improved and precise study of more suppressed $b \to dll$ decays.

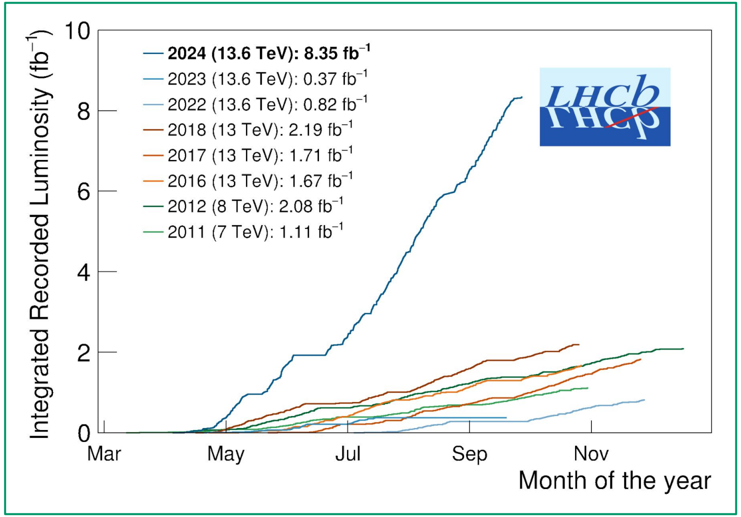

STAY TUNED!

Back-up

Probing New Physics (NP)

1. Direct searches (LHC):
   limited by $E = mc^2$, no discovery so far

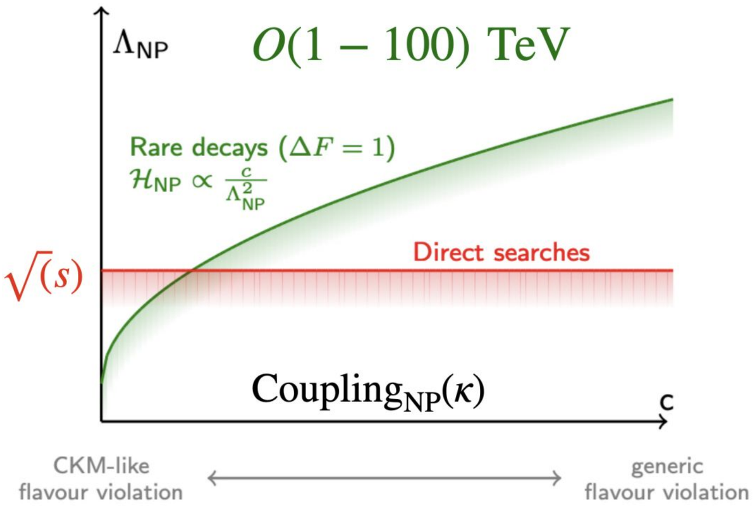

2. **Precision measurements**
   - experimentally accessible
   - suppressed processes ⇒ very sensitive to (small) NP effects
   - precise predictions ⇒ smoking gun of NP

Flavour Changing Neutral Currents (FCNC)

LHCb: Large Hadron Collider Beauty experiment

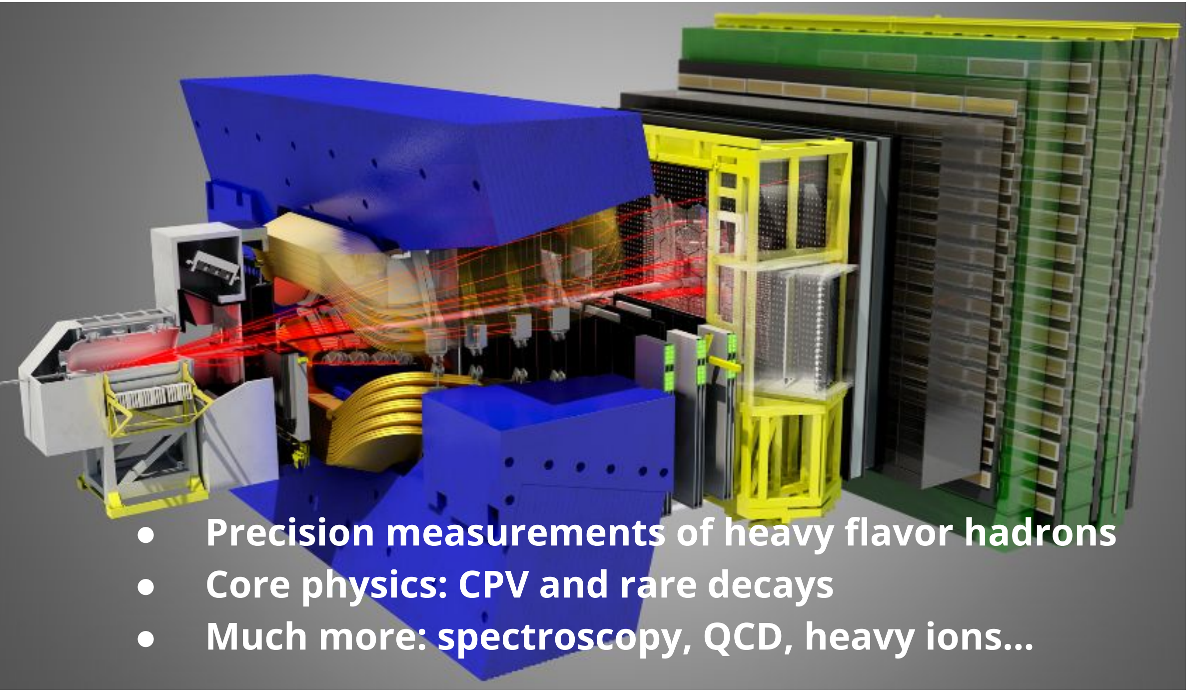

- Precision measurements of heavy flavor hadrons
- Core physics: CPV and rare decays
- Much more: spectroscopy, QCD, heavy ions...

Distribution of produced b-quarks

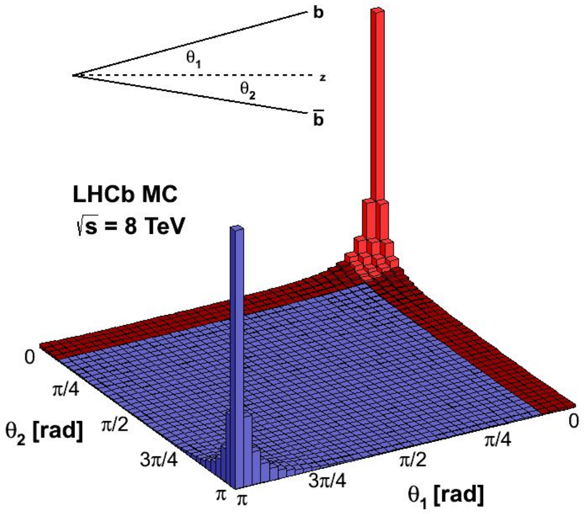

JINST 3 (2008) S08005

LHCb dataset

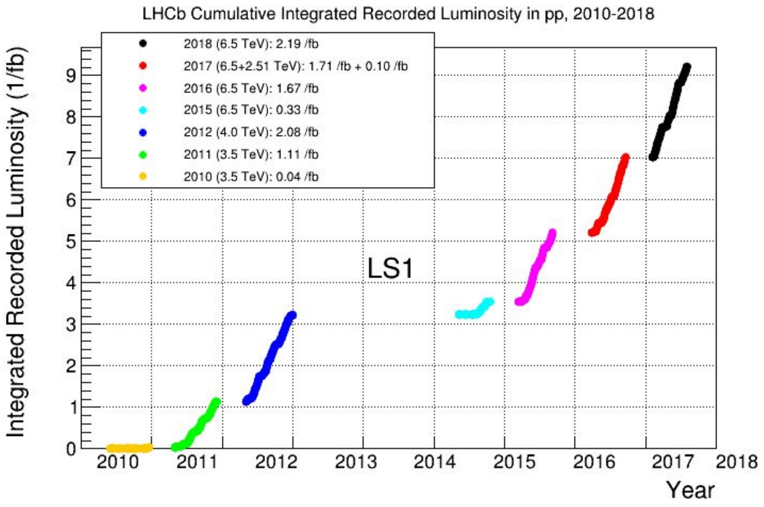

All b-hadron species! [PRD100(2019)031102]

- B_s: $\frac{f_s}{f_d+f_u} = 0.122 \pm 0.006$
- Λ_b: $\frac{f_{\Lambda_b}}{f_d+f_u} = 0.259 \pm 0.018$

and more: Ξ_b, Ω_b, B_c, B^* ...

Total recorded luminosity ~9 fb^{-1}:

- Run 1 (2010-2012) ~ 3 fb^{-1}
- Run 2 (2015-2018) ~ 6 fb^{-1}

x2 b-quark production from 7 to 13 TeV pp collisions
→ around x4 b-hadrons in Run 2

Angle definitions

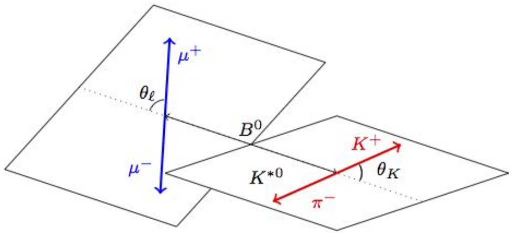

(a) θ_K and θ_ℓ definitions for the B^0 decay

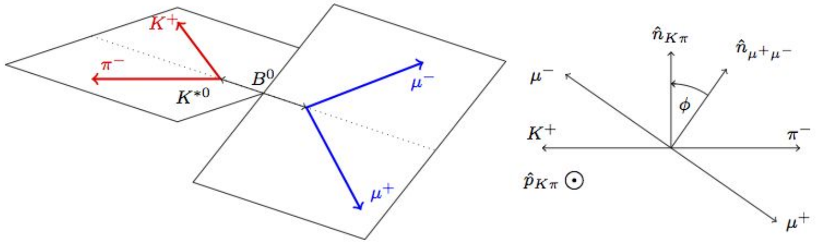

(b) ϕ definition for the B^0 decay

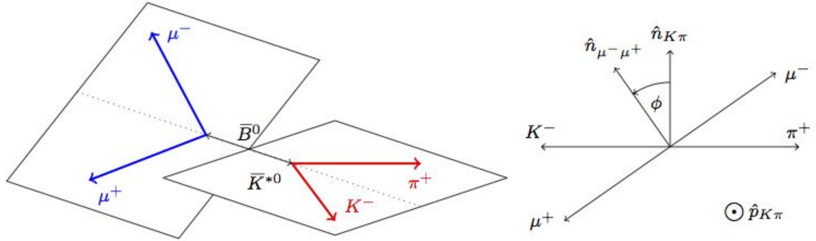

(c) ϕ definition for the $\overline{B}^0$ decay

$\Lambda_b \to pK\mu^+\mu^-$

- Unpolarised Λ_b
- J_Λ <= 5/2

BF extraction wrt J/ψ mode:

$$\frac{\mathrm{d}^2\mathcal{B}(\Lambda_b^0 \to pK^-\mu^+\mu^-)}{\mathrm{d}q^2\mathrm{d}m_{pK}^2} = \frac{N_{\Lambda_b^0\to pK^-\mu^+\mu^-}}{N_{\Lambda_b^0\to J/\psi pK^-}} \frac{\mathcal{B}(\Lambda_b^0 \to J/\psi pK^-)\mathcal{B}(J/\psi \to \mu^+\mu^-)}{\Delta(q^2, m_{pK}^2)}$$

Efficiency model:

$$\varepsilon(\Phi) = \sum_{hijkl} e_{hijkl} P_h(m'_{pK}) P_i(m'_{\mu\mu}) P_j(\cos\theta_p) P_k(\cos\theta_\mu)\cos(l\phi)$$

i	$f_i(\Omega)$	i	$f_i(\Omega)$
1	$\frac{1}{\sqrt{3}}P_0^0(\cos\theta_p)P_0^0(\cos\theta_\mu)$	24	$\frac{1}{2}\sqrt{\frac{7}{3}}P_3^1(\cos\theta_p)P_1^1(\cos\theta_\mu)\cos\phi$
2	$P_0^0(\cos\theta_p)P_1^0(\cos\theta_\mu)$	25	$\frac{1}{2}P_4^1(\cos\theta_p)P_2^1(\cos\theta_\mu)\cos\phi$
3	$\sqrt{\frac{5}{3}}P_0^0(\cos\theta_p)P_2^0(\cos\theta_\mu)$	26	$\frac{3}{2\sqrt{5}}P_4^1(\cos\theta_p)P_1^1(\cos\theta_\mu)\cos\phi$
4	$P_1^0(\cos\theta_p)P_0^0(\cos\theta_\mu)$	27	$\frac{1}{3}\sqrt{\frac{11}{6}}P_5^1(\cos\theta_p)P_2^1(\cos\theta_\mu)\cos\phi$
5	$\sqrt{3}P_1^0(\cos\theta_p)P_1^0(\cos\theta_\mu)$	28	$\sqrt{\frac{11}{30}}P_5^1(\cos\theta_p)P_1^1(\cos\theta_\mu)\cos\phi$
6	$\sqrt{5}P_1^0(\cos\theta_p)P_2^0(\cos\theta_\mu)$	29	$\sqrt{\frac{5}{6}}P_1^1(\cos\theta_p)P_2^1(\cos\theta_\mu)\sin\phi$
7	$\sqrt{\frac{5}{3}}P_2^0(\cos\theta_p)P_0^0(\cos\theta_\mu)$	30	$\sqrt{\frac{3}{2}}P_1^1(\cos\theta_p)P_1^1(\cos\theta_\mu)\sin\phi$
8	$\sqrt{5}P_2^0(\cos\theta_p)P_1^0(\cos\theta_\mu)$	31	$\frac{5}{3\sqrt{6}}P_2^1(\cos\theta_p)P_2^1(\cos\theta_\mu)\sin\phi$
9	$\frac{5}{\sqrt{3}}P_2^0(\cos\theta_p)P_2^0(\cos\theta_\mu)$	32	$\sqrt{\frac{5}{6}}P_2^1(\cos\theta_p)P_1^1(\cos\theta_\mu)\sin\phi$
10	$\sqrt{\frac{7}{3}}P_3^0(\cos\theta_p)P_0^0(\cos\theta_\mu)$	33	$\frac{1}{6}\sqrt{\frac{35}{3}}P_3^1(\cos\theta_p)P_2^1(\cos\theta_\mu)\sin\phi$
11	$\sqrt{7}P_3^0(\cos\theta_p)P_1^0(\cos\theta_\mu)$	34	$\frac{1}{2}\sqrt{\frac{7}{3}}P_3^1(\cos\theta_p)P_1^1(\cos\theta_\mu)\sin\phi$
12	$\sqrt{\frac{35}{3}}P_3^0(\cos\theta_p)P_2^0(\cos\theta_\mu)$	35	$\frac{1}{2}P_4^1(\cos\theta_p)P_2^1(\cos\theta_\mu)\sin\phi$
13	$\sqrt{3}P_4^0(\cos\theta_p)P_0^0(\cos\theta_\mu)$	36	$\frac{3}{2\sqrt{5}}P_4^1(\cos\theta_p)P_1^1(\cos\theta_\mu)\sin\phi$
14	$3P_4^0(\cos\theta_p)P_1^0(\cos\theta_\mu)$	37	$\frac{1}{3}\sqrt{\frac{11}{6}}P_5^1(\cos\theta_p)P_2^1(\cos\theta_\mu)\sin\phi$
15	$\sqrt{15}P_4^0(\cos\theta_p)P_2^0(\cos\theta_\mu)$	38	$\sqrt{\frac{11}{30}}P_5^1(\cos\theta_p)P_1^1(\cos\theta_\mu)\sin\phi$
16	$\sqrt{\frac{11}{3}}P_5^0(\cos\theta_p)P_0^0(\cos\theta_\mu)$	39	$\frac{5}{12\sqrt{6}}P_2^2(\cos\theta_p)P_2^2(\cos\theta_\mu)\cos 2\phi$
17	$\sqrt{11}P_5^0(\cos\theta_p)P_1^0(\cos\theta_\mu)$	40	$\frac{1}{12}\sqrt{\frac{7}{6}}P_3^2(\cos\theta_p)P_2^2(\cos\theta_\mu)\cos 2\phi$
18	$\sqrt{\frac{55}{3}}P_5^0(\cos\theta_p)P_2^0(\cos\theta_\mu)$	41	$\frac{1}{12\sqrt{2}}P_4^2(\cos\theta_p)P_2^2(\cos\theta_\mu)\cos 2\phi$
19	$\sqrt{\frac{5}{6}}P_1^1(\cos\theta_p)P_2^1(\cos\theta_\mu)\cos\phi$	42	$\frac{1}{12}\sqrt{\frac{11}{42}}P_5^2(\cos\theta_p)P_2^2(\cos\theta_\mu)\cos 2\phi$
20	$\sqrt{\frac{3}{2}}P_1^1(\cos\theta_p)P_1^1(\cos\theta_\mu)\cos\phi$	43	$\frac{5}{12\sqrt{6}}P_2^2(\cos\theta_p)P_2^2(\cos\theta_\mu)\sin 2\phi$
21	$\frac{5}{3\sqrt{6}}P_2^1(\cos\theta_p)P_2^1(\cos\theta_\mu)\cos\phi$	44	$\frac{1}{12}\sqrt{\frac{7}{6}}P_3^2(\cos\theta_p)P_2^2(\cos\theta_\mu)\sin 2\phi$
22	$\sqrt{\frac{5}{6}}P_2^1(\cos\theta_p)P_1^1(\cos\theta_\mu)\cos\phi$	45	$\frac{1}{12\sqrt{2}}P_4^2(\cos\theta_p)P_2^2(\cos\theta_\mu)\sin 2\phi$
23	$\frac{1}{6}\sqrt{\frac{35}{3}}P_3^1(\cos\theta_p)P_2^1(\cos\theta_\mu)\cos\phi$	46	$\frac{1}{12}\sqrt{\frac{11}{42}}P_5^2(\cos\theta_p)P_2^2(\cos\theta_\mu)\sin 2\phi$

$\Lambda_b \to pK\mu^+\mu^-$ mass fits

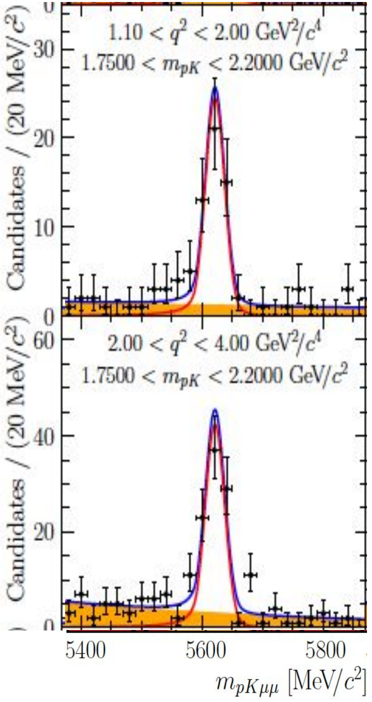

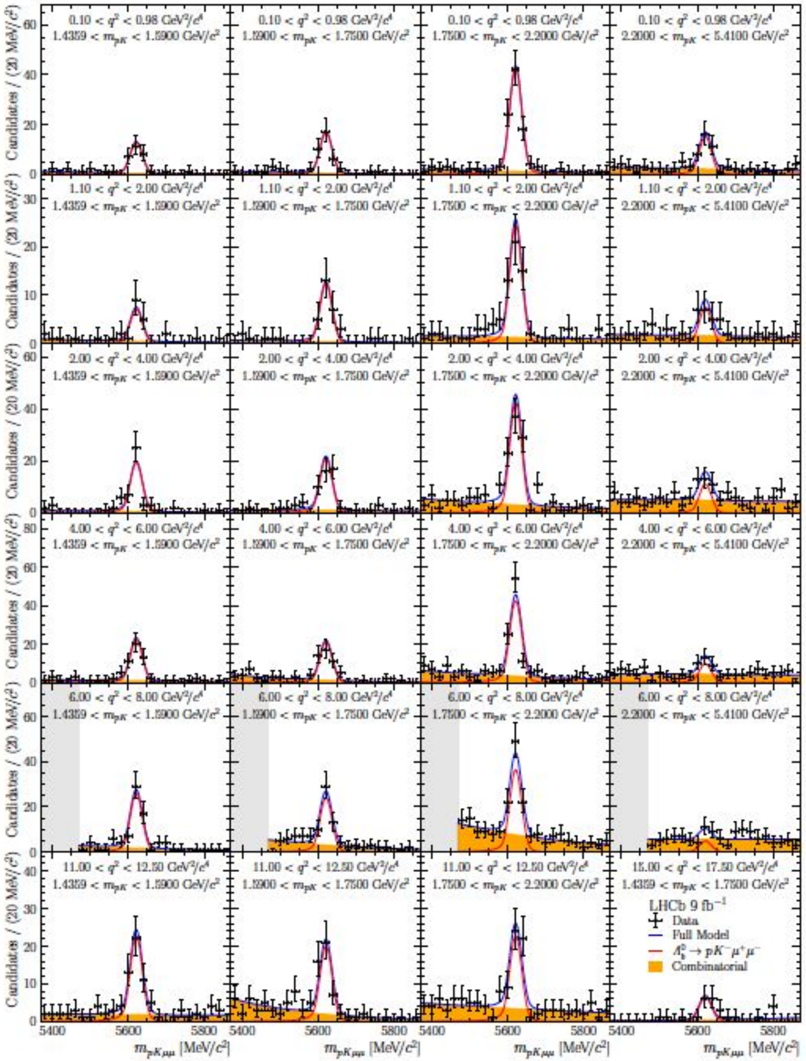

Angular observables

Range of observables sensitive to different WCs

$$\frac{1}{\mathrm{d}(\Gamma+\bar{\Gamma})/\mathrm{d}q^2}\frac{\mathrm{d}^4(\Gamma+\bar{\Gamma})}{\mathrm{d}q^2\,\mathrm{d}\vec{\Omega}}\Big|_{\mathrm{P}} = \frac{9}{32\pi}\Big[\tfrac{3}{4}(1-F_{\mathrm{L}})\sin^2\theta_K + F_{\mathrm{L}}\cos^2\theta_K + \tfrac{1}{4}(1-F_{\mathrm{L}})\sin^2\theta_K\cos 2\theta_l - F_{\mathrm{L}}\cos^2\theta_K\cos 2\theta_l + S_3\sin^2\theta_K\sin^2\theta_l\cos 2\phi + S_4\sin 2\theta_K\sin 2\theta_l\cos\phi + S_5\sin 2\theta_K\sin\theta_l\cos\phi + \tfrac{4}{3}A_{\mathrm{FB}}\sin^2\theta_K\cos\theta_l + S_7\sin 2\theta_K\sin\theta_l\sin\phi + S_8\sin 2\theta_K\sin 2\theta_l\sin\phi + S_9\sin^2\theta_K\sin^2\theta_l\sin 2\phi\Big]$$

$B_d \rightarrow K^* \mu^+ \mu^-$

[Altmannshofer et al.]

F_L: H longitudinal polarisation

A_{FB}: di-lepton forward-backward asymmetry

S_i: CP-averaged observables

"Clean" basis: cancellation of Form Factors at leading order [Descotes-Genon et al.]

$$P_5' = S_5/\sqrt{F_{\mathrm{L}}(1-F_{\mathrm{L}})}$$

$B^0 \to K^*\mu^+\mu^-$: angular coefficients

$$J_{1s}(q^2) = \frac{2+\beta_\ell^2}{4}\left(|\mathcal{A}_\perp^L|^2 + |\mathcal{A}_\parallel^L|^2 + |\mathcal{A}_\perp^R|^2 + |\mathcal{A}_\parallel^R|^2\right) + \frac{4m_\ell^2}{q^2}\,\mathrm{Re}\left(\mathcal{A}_\perp^L\mathcal{A}_\perp^{R*} + \mathcal{A}_\parallel^L\mathcal{A}_\parallel^{R*}\right),$$

$$J_{1c}(q^2) = |\mathcal{A}_0^L|^2 + |\mathcal{A}_0^R|^2 + \frac{4m_\ell^2}{q^2}\left(|\mathcal{A}_t|^2 + 2\,\mathrm{Re}\left(\mathcal{A}_0^L\mathcal{A}_0^{R*}\right)\right),$$

$$J_{2s}(q^2) = \frac{\beta_\ell^2}{4}\left(|\mathcal{A}_\perp^L|^2 + |\mathcal{A}_\parallel^L|^2 + |\mathcal{A}_\perp^R|^2 + |\mathcal{A}_\parallel^R|^2\right),$$

$$J_{2c}(q^2) = -\beta_\ell^2\left(|\mathcal{A}_0^L|^2 + |\mathcal{A}_0^R|^2\right),$$

$$J_3(q^2) = \frac{\beta_\ell^2}{2}\left(|\mathcal{A}_\perp^L|^2 - |\mathcal{A}_\parallel^L|^2 + |\mathcal{A}_\perp^R|^2 - |\mathcal{A}_\parallel^R|^2\right),$$

$$J_4(q^2) = -\frac{\beta_\ell^2}{\sqrt{2}}\,\mathrm{Re}\left(\mathcal{A}_0^L\mathcal{A}_\parallel^{L*} + \mathcal{A}_0^R\mathcal{A}_\parallel^{R*}\right),$$

$$J_5(q^2) = \sqrt{2}\beta_\ell\,\mathrm{Re}\left(\mathcal{A}_0^L\mathcal{A}_\perp^{L*} - \mathcal{A}_0^R\mathcal{A}_\perp^{R*}\right),$$

$$J_{6s}(q^2) = -2\beta_\ell\,\mathrm{Re}\left(\mathcal{A}_\parallel^L\mathcal{A}_\perp^{L*} - \mathcal{A}_\parallel^R\mathcal{A}_\perp^{R*}\right),$$

$$J_7(q^2) = -\sqrt{2}\beta_\ell\,\mathrm{Im}\left(\mathcal{A}_0^L\mathcal{A}_\parallel^{L*} - \mathcal{A}_0^R\mathcal{A}_\parallel^{R*}\right),$$

$$J_8(q^2) = \frac{\beta_\ell^2}{\sqrt{2}}\,\mathrm{Im}\left(\mathcal{A}_0^L\mathcal{A}_\perp^{L*} + \mathcal{A}_0^R\mathcal{A}_\perp^{R*}\right),$$

$$J_9(q^2) = -\beta_\ell^2\,\mathrm{Im}\left(\mathcal{A}_\parallel^{L*}\mathcal{A}_\perp^L + \mathcal{A}_\parallel^{R*}\mathcal{A}_\perp^R\right),$$

$$J_{1c}^{S'}(q^2) = \frac{1}{3}\left(\left(|\mathcal{A}_{00}^L|^2 + |\mathcal{A}_{00}^R|^2\right) + \frac{4m_\ell^2}{q^2}2\,\mathrm{Re}(\mathcal{A}_{00}^L\mathcal{A}_{00}^{R*})\right),$$

$$J_{2c}^{S'}(q^2) = -\frac{1}{3}\beta_\ell^2\left(|\mathcal{A}_{00}^L|^2 + |\mathcal{A}_{00}^R|^2\right),$$

$$J'_{1c}(q^2) = \frac{2}{\sqrt{3}}\,\mathrm{Re}\left(\mathcal{A}_{00}^L\mathcal{A}_0^{L*} + \mathcal{A}_{00}^R\mathcal{A}_0^{R*} + \frac{4m_\ell^2}{q^2}\left(\mathcal{A}_{00}^L\mathcal{A}_0^{R*} + \mathcal{A}_0^L\mathcal{A}_{00}^{R*}\right)\right),$$

$$J'_{2c}(q^2) = -\frac{2}{\sqrt{3}}\beta_\ell^2\,\mathrm{Re}\left(\mathcal{A}_{00}^L\mathcal{A}_0^{L*} + \mathcal{A}_{00}^R\mathcal{A}_0^{R*}\right),$$

$$J'_4(q^2) = -\sqrt{\frac{2}{3}}\beta_\ell^2\left(\mathrm{Re}\left(\mathcal{A}_{00}^L\mathcal{A}_\parallel^{L*}\right) + \mathrm{Re}\left(\mathcal{A}_{00}^R\mathcal{A}_\parallel^{R*}\right)\right),$$

$$J'_5(q^2) = 2\sqrt{\frac{2}{3}}\beta_\ell^2\left(\mathrm{Re}\left(\mathcal{A}_{00}^L\mathcal{A}_\perp^{L*}\right) + \mathrm{Re}\left(\mathcal{A}_{00}^R\mathcal{A}_\perp^{R*}\right)\right),$$

$$J'_7(q^2) = -2\sqrt{\frac{2}{3}}\beta_\ell^2\left(\mathrm{Re}\left(\mathcal{A}_{00}^L\mathcal{A}_\parallel^{L*}\right) - \mathrm{Re}\left(\mathcal{A}_{00}^R\mathcal{A}_\parallel^{R*}\right)\right),$$

$$J'_8(q^2) = \sqrt{\frac{2}{3}}\beta_\ell^2\left(\mathrm{Re}\left(\mathcal{A}_{00}^L\mathcal{A}_\perp^{L*}\right) - \mathrm{Re}\left(\mathcal{A}_{00}^R\mathcal{A}_\perp^{R*}\right)\right).$$

$B^0 \to K^*\mu^+\mu^-$ Fit projections

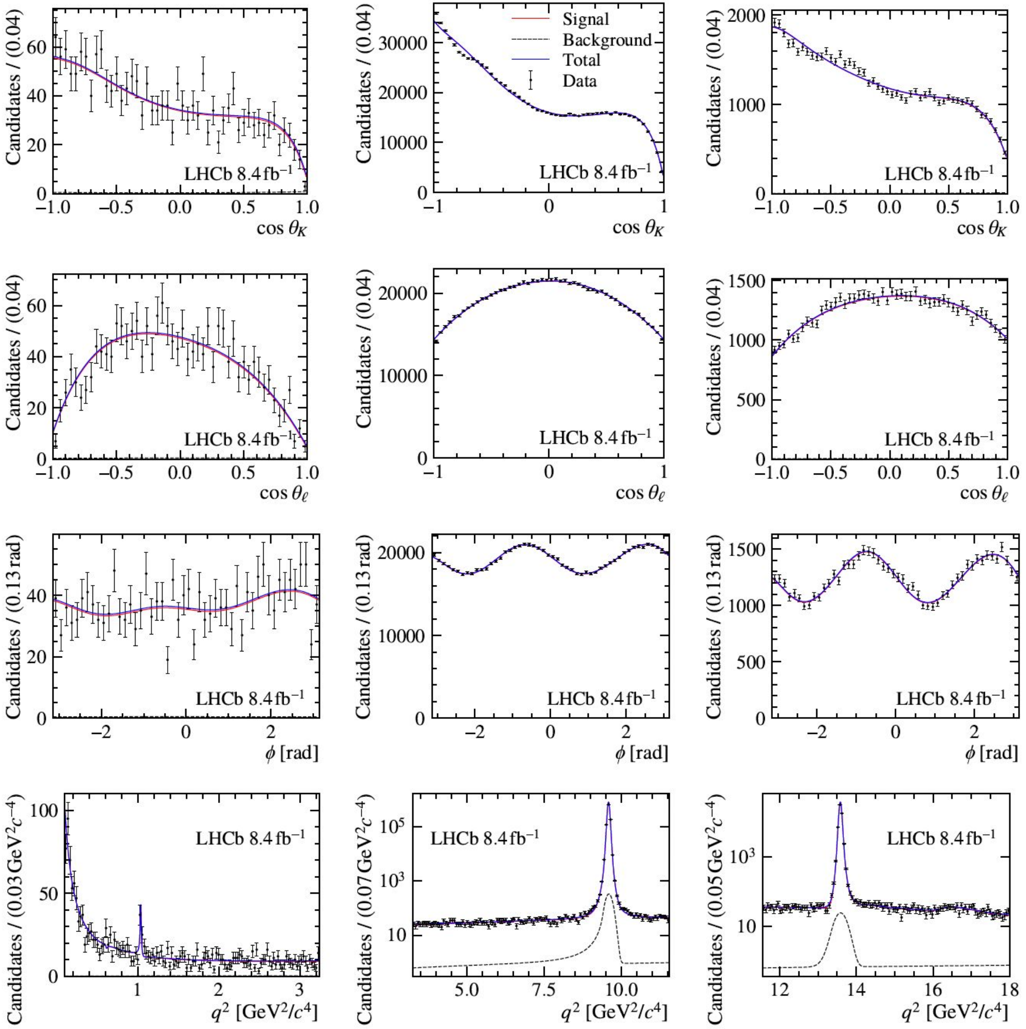

$B^0 \longrightarrow K^{*}\mu^{+}\mu^{-}$: acceptance

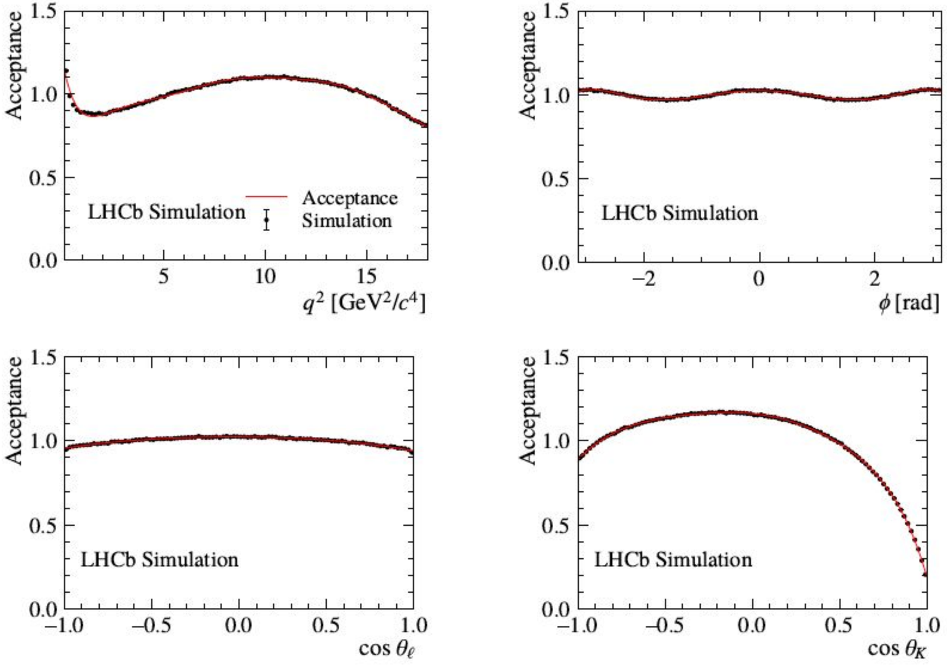

Figure 1: One-dimensional projections of the acceptance function determined from simulation.

$B^0 \to K^*\mu^+\mu^-$ Local FF

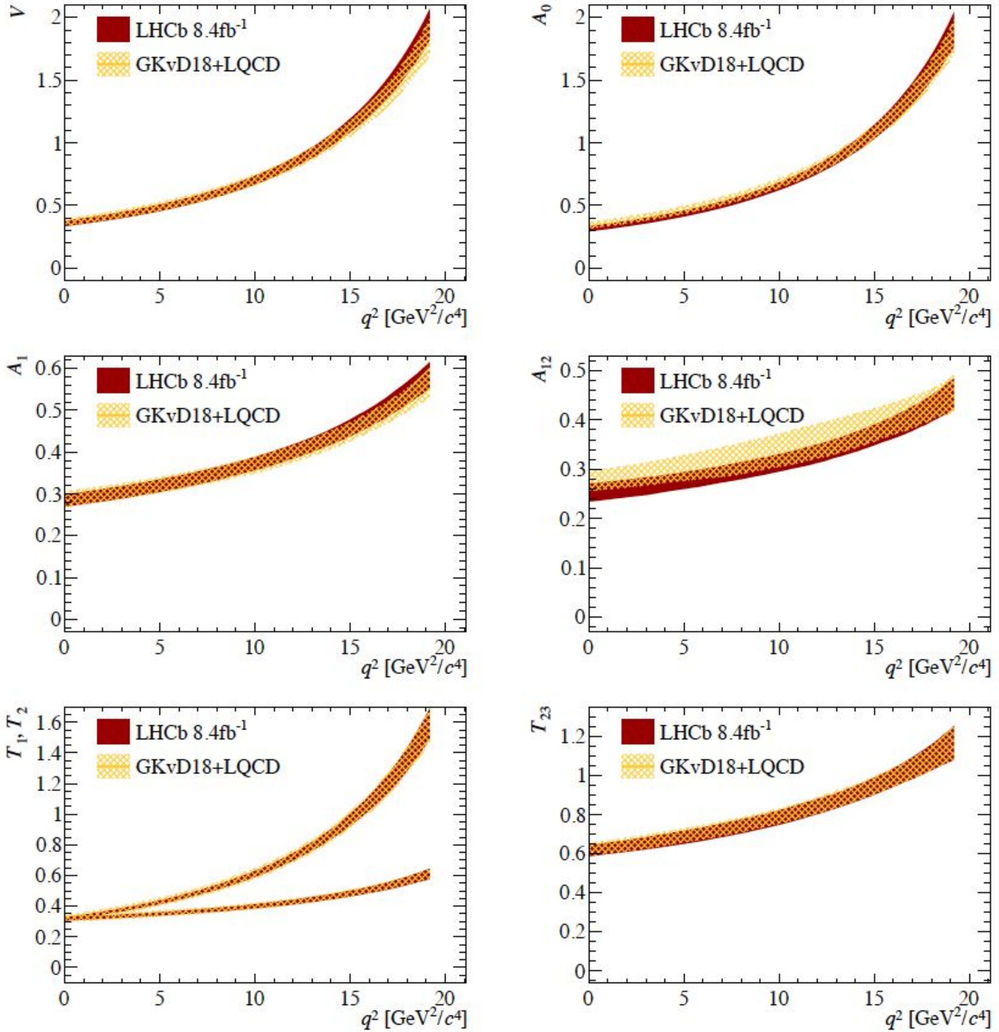

$B^0 \to K^*\mu^+\mu^-$: Nonlocal contribution

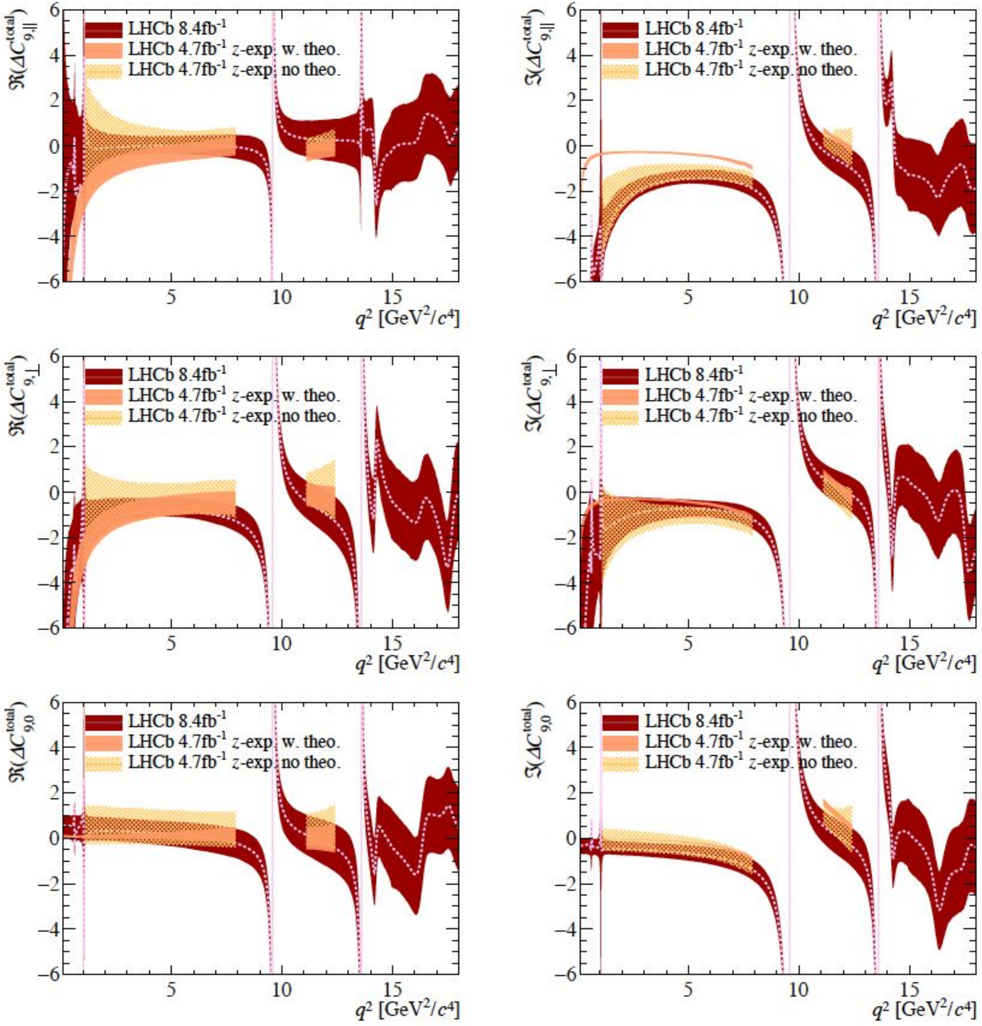

Challenges: hardware trigger

ECAL occupancy > Muon one
⇒ tighter thresholds for electrons:

- **e p_T** > 2700/2400 MeV in 2012/2016
- **μ p_T** > 1700/1800 MeV in 2012/2016

[LHCb-PUB-2014-046, 2019 JINST 14 P04013]

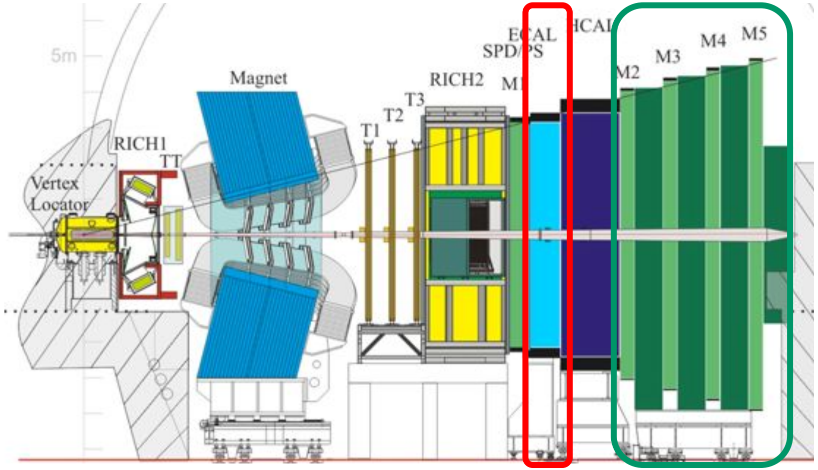

Mitigation:

- events triggered independently of the signal (TIS)
- (hadron trigger)

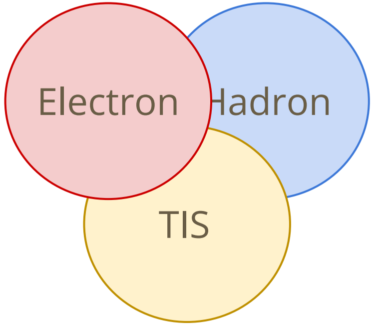

Challenges: material interactio

Electrons radiate much more
Bremsstrahlung → recovery procedure:

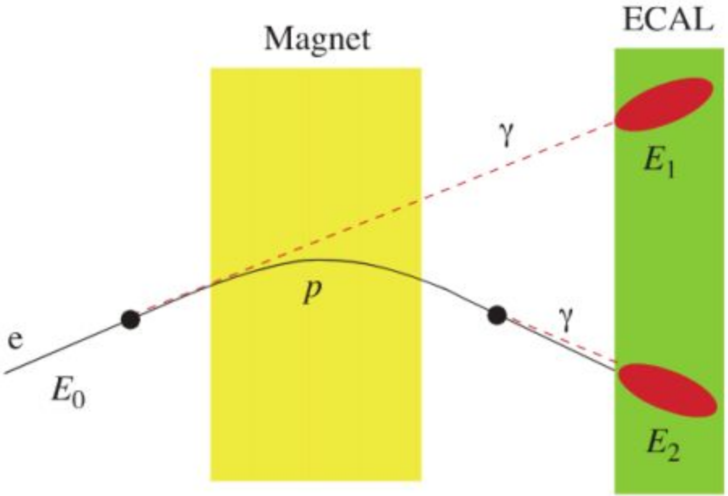

Limitations:

- miss some photons and add fake ones
- ECAL resolution worse than tracking

→ worse mass resolution for electron modes
→ more and larger backgrounds
→ more complicated mass fit

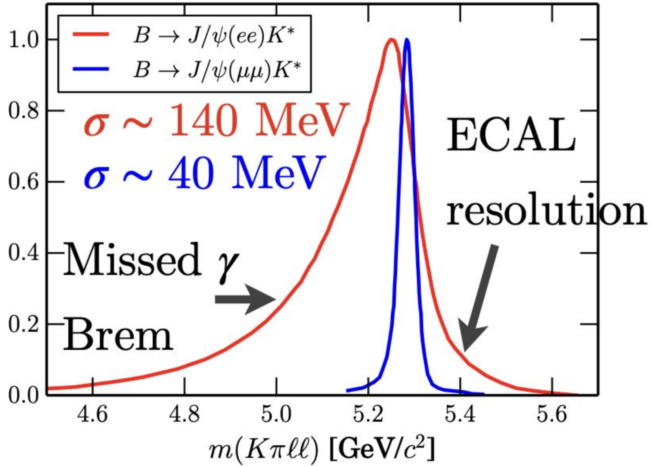

How do we control the efficiencies?

Exploit J/ψ modes to build double ratio to cancel systematic effects

$$R_H = \frac{\dfrac{N(B\to H\mu^+\mu^-)}{N(B\to HJ/\psi(\mu^+\mu^-))}}{\dfrac{N(B\to He^+e^-)}{N(B\to HJ/\psi(e^+e^-))}} \times \frac{\dfrac{\epsilon(B\to He^+e^-)}{\epsilon(B\to HJ/\psi(e^+e^-))}}{\dfrac{\epsilon(B\to H\mu^+\mu^-)}{\epsilon(B\to HJ/\psi(\mu^+\mu^-))}}$$

LFU well tested in J/ψ modes → stringent cross-check

$$r_{J/\psi} = \frac{N(B\to HJ/\psi(\mu^+\mu^-))}{N(B\to HJ/\psi(e^+e^-))} \times \frac{\epsilon(B\to HJ/\psi(e^+e^-))}{\epsilon(B\to HJ/\psi(\mu^+\mu^-))}$$

Measurement of R_K and R_{K^*}

$B^+ \to K^+ll$ and $B^0 \to K^*ll$ studied simultaneously

- two q^2 bins: [0.1, 1.1] (low) and [1.1, 6] GeV^2 (central)
- $m(K^+\pi^-) \in [792, 992]$ MeV for $B^0 \to K^*ll$

Main improvements:

- constraint cross-feed backgrounds from data
- tighter $e^\pm$ PID selection
- specific modelling of $e^\pm$ misID background

Details in arXiv:2212.09152 and arXiv:2212.09153

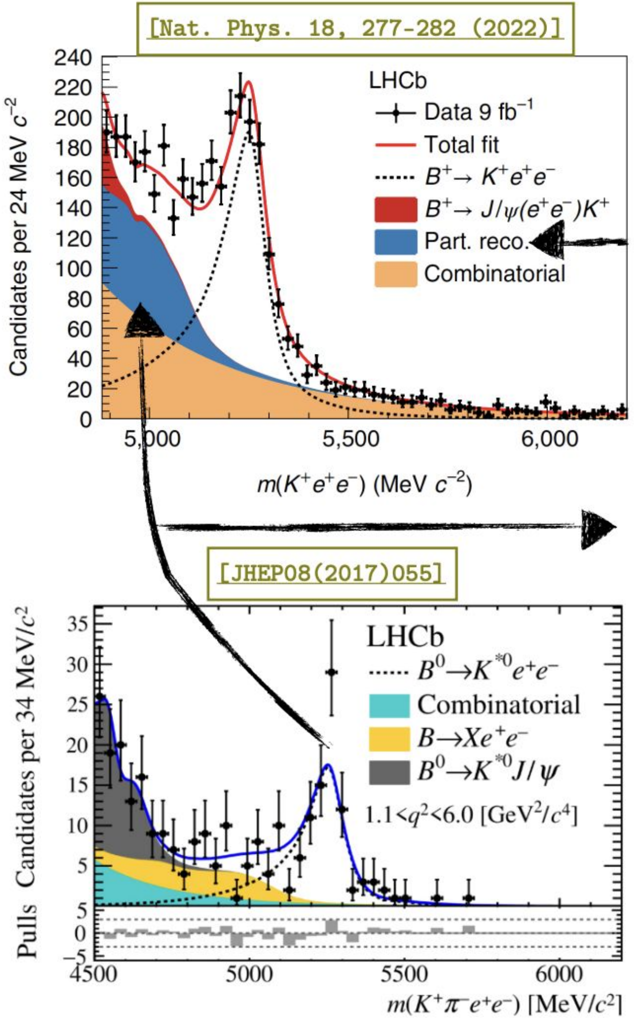

arXiv:2212.09153

Measurement of R_K and R_{K^*}

Simultaneous fit to low, central and J/ψ regions; K and K^*; and $\mu^\pm$ and $e^\pm$

- R_K central q^2:

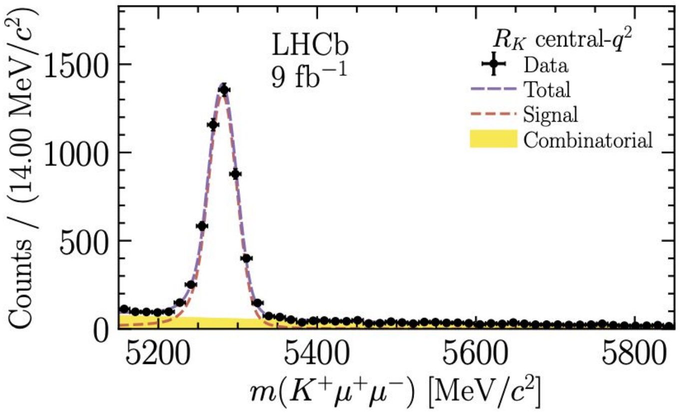

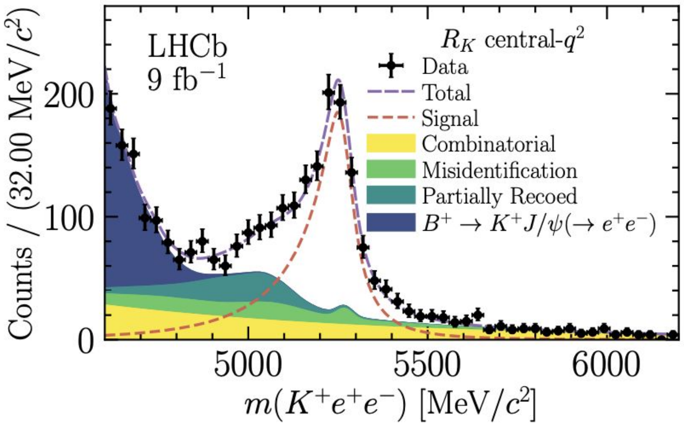

arXiv:2212.09153

Measurement of R_K and R_{K^*}

Results of four simultaneous measurements:

- Compatible with SM at 0.2σ
- Final result of Run 2 on R_{K,K^*}
- Muon BR agrees with prev. results

$$\text{low-}q^2 \begin{cases} R_K = 0.994\ ^{+0.090}_{-0.082}\ (\text{stat})\ ^{+0.027}_{-0.029}\ (\text{syst}), \\ R_{K^*} = 0.927\ ^{+0.093}_{-0.087}\ (\text{stat})\ ^{+0.034}_{-0.033}\ (\text{syst}) \end{cases}$$

$$\text{central-}q^2 \begin{cases} R_K = 0.949\ ^{+0.042}_{-0.041}\ (\text{stat})\ ^{+0.023}_{-0.023}\ (\text{syst}), \\ R_{K^*} = 1.027\ ^{+0.072}_{-0.068}\ (\text{stat})\ ^{+0.027}_{-0.027}\ (\text{syst}). \end{cases}$$